EXPERIMENTAL SPACE WEATHERING OF ORDINARY CHONDRITES BY NANOPULSE LASER: TEM RESULTS.

S. K. Noble[1], T. Hiroi[2], L. P. Keller[3], Z. Rahman[3], S. Sasaki[4], and C. M. Pieters[2] [1]NASA GSFC Mail Code 691, Greenbelt MD 20771, sarah.k.noble@nasa.gov, [2]Brown University, 324 Brook Street, Providence RI 02912, takihiroi@gmail.com, [3]NASA Johnson Space Center, Houston TX, 77058, [4]RISE Project, National Astronomical Observatory of Japan, Oshu City, Japan

Introduction: A set of ordinary chondrite meteorites has been subjected to artificial space weathering by nanopulse laser to simulate the effects of micrometeorite bombardment. Three meteorites, an H (Ehole), L (Chateau Renard - CR), and LL (Appley Bridge - AB) were lasered following the method of Sasaki et al [1]. Near IR spectra were taken before and after exposure to examine the optical changes induced and the samples were examined by scanning and transmission electron microscopy (SEM and TEM) to understand the physical changes.

Background: The effects of space weathering on a given body are dependent on many factors including the physical conditions and chemical composition of the target material. One way to understand those relationships is to simulate space weathering in the laboratory. It has already been shown that irradiation with a nanopulse laser results in the formation of npFe° and the VIS-NIR spectral reddening and darkening that are the hallmarks of space weathering [1]. Here we are looking at a series of meteorites with a range of metallic iron to understand what effect, if any, that has on the weathering products produced.

Space weathering has traditionally been thought of as a soil process, but exposed rocks will also incur the effects of space weathering. Weathering patinas have been described on lunar rocks [2, 3], but mature outcrops are only small contributors to the lunar spectrum on a remote sensing scale. Results from the Hayabusa spacecraft at the asteroid Itokowa suggest that while the low gravity does not allow for the development of a mature regolith, weathering patinas can and do develop on rock surfaces [4], thus for small bodies, rock weathering may be an important process.

Vis-NIR Spectra: Diffuse visible-NIR reflectance spectra were measured at 30 degree incidence and 0 degree emergence angles using spectrometers located either at RELAB, Brown University or in Mizusawa Campus of the National Observatory of Japan.

As previous experiments on individual minerals have shown, the lasered samples follow typical space weathering trends, becoming darker, redder, and losing spectral contrast with increasing laser exposure (Fig 1).

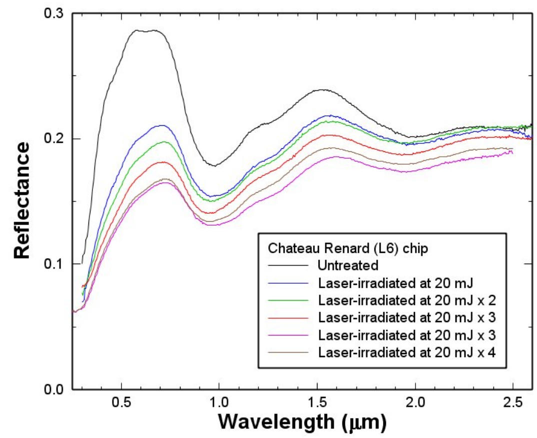

Figure 1. Spectra from a chip of the L6 meteorite Chateau Renard before and after exposure to the laser.

SEM results: The samples were studied under scanning electron microscope to understand the textural changes induced by the laser pulses and to select areas of interest for TEM analysis. All three samples display evidence of melting where the laser made contact. Fig 2 is a good example of localized melting induced by a single laser pulse. The affected areas tend to be highly vesicular. Different degrees of melting are evident for different minerals. Sulfides, like the bright material in Fig 2, and Ni-Fe tend to not only melt, but disperse in small ~1-5 μm droplets. In Fig 3 there is a sharp contrast between the darker plagioclase, which appears unmelted, and the brighter pyroxene, which displays a highly vesiculated melt texture.

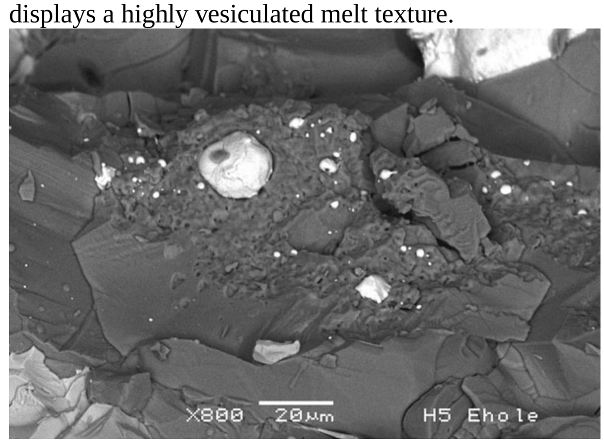

Figure 2. Nanopulse laser induced effects on plagioclase and iron sulfide in the H5 meteorite Ehole.

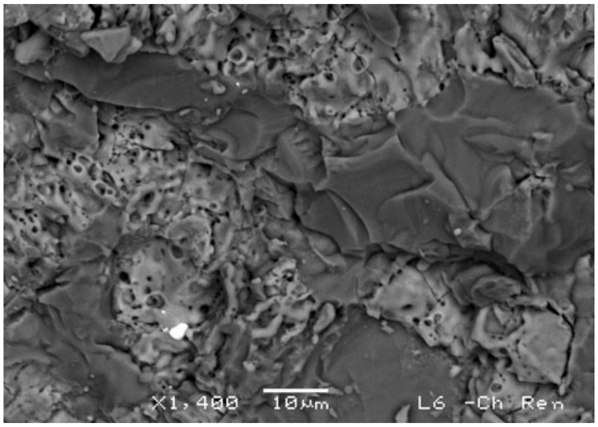

Figure 3. While the pyroxene (lighter material) shows signs of significant melting, the plagioclase does not.

TEM results: Focused ion beam (FIB) methods were used to extract a single sample from each of the three meteorites for the TEM. The samples were analyzed using the JEOL 2500SE 200 keV field-emission scanning-transmission electron microscope (FE-STEM) at JSC. The FE-STEM is equipped with a large-area, thin window energy-dispersive X-ray (EDX) spectrometer.

In Figs 4 and 5 below are images and maps created from the H5 (Ehole) and L5 (CR) FIB sections. No obvious differences were detected in the melt/vapor layers between the 3 types. NpFe° is present in similar size and abundance in all three samples. The main difference between the samples seems to relate largely to their shock state; while both CR and AB have abundant cracks and fractures that were exploited by the melt, Ehole is nearly fracture-free and its melt/vapor layer is nearly uniform. Both Ehole and CR have melt splats on top of their melt/vapor layers; this appears to be common based on the SEM imagery, particularly for sulfides and NiFe (see fig 2). It is also a process commonly seen in the weathering patina of lunar rocks [2, 3].

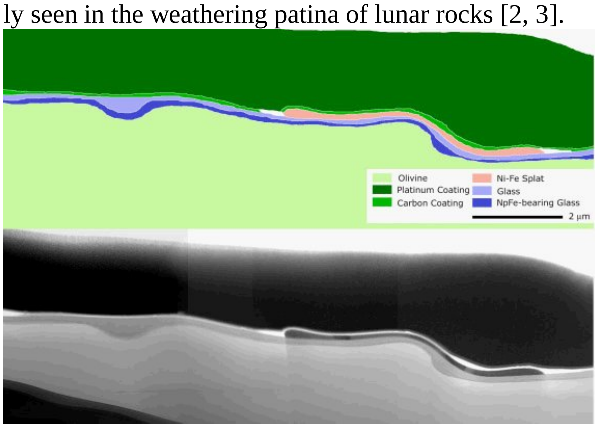

Figure 4. Map (top) and bright field image of Ehole (H5) after nanopulse laser.

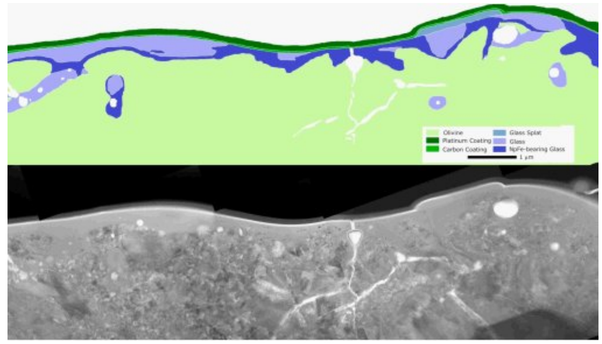
Figure 5. Map (top) and bright field image of Chateau Renard (L5) after nanopulse laser.

While Ehole's melt/vapor layer (Fig 6) was the most uniform, all showed similar trends. All three samples contained a melt layer ~100-500 nm thick, with npFe° largely concentrated in the bottom half of the melt layer. The average size of these npFe° grains in Ehole is 5 nm, with a range of about 2 to 15, this is consistent with npFe° seen in lunar soil rims, which ranges from about 1-15 nm with an average of 3 nm [5]. In some places, a thin (~20 nm) vapor-deposited layer can be seen at the top surface. This layer, when present, is enriched in sulfur and is also npFe°-rich, though the iron is smaller, ~1-3 µm.

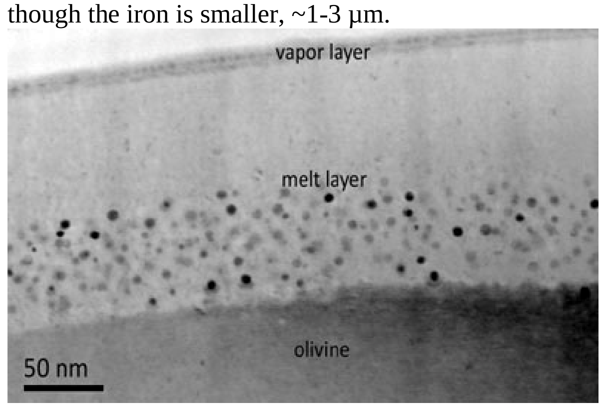

Figure 6. TEM bright field image of melt/vapor layer of Ehole.

Conclusions: TEM analysis of artificially space weathered ordinary chondrites with different metallic iron contents reveals the creation of similar npFe°-bearing melt and vapor deposits.

References: [1] Sasaki et al. (2001) *Nature, 410*, #6828, 555-557. [2] Wentworth S. J. et al. (1999) *MaPS, 34*, 593-603. [3] Noble et al (2007) *LPSC XXXVIII*, Abstract #1359. [4] Hiroi et al (2006) *Nature 443*, 56-58. [5] Keller L. P. and Clemett S. J. (2001) *LPSC XXXII*, Abstract #2097.

Acknowledgments: Support for T. Hiroi from NASA's DDAP is greatfully acknowledged. Electron microscopy and FIB prep were performed in the Electron Beam Analysis Labs at NASA/JSC.